JOURNAL OF HIGH-FREQUENCY COMMUNICATION TECHNOLOGIES
Vol. 01 (03) (2023), pp.84-101. ***e-ISSN:2836-9009***
https://doi.org/10.58399/LUSI2152

Intelligent Encoding through OCDM for High Capacity and Connectivity in Wireless 5G and Beyond Networks

S.Brindha[1*], T.Ilavarasan[2], T.Sivasakthi[3], G.Lakshmi[4], A.Rashmi[5], Sanjiv Kumar Saminathan[6], M.Meenakshi[7]

[1,3,4,5] Department of ECE, Sri Sairam Engineering college, Chennai-600 044, India

E-mail address: sbrindha.ece@sairam.edu.in, sivasakthi.ece@sairam.edu.in, lakshmig237@gmail.com, rashmichitra27@gmail.com

[2]Deptartment of ECE, Vellore Institute of Technology, Chennai, Tamil Nadu – 600 127, India
E-mail address: ila.ece@gmail.com

[6]Deptartment of Biotechnology, Indian Institute of Technology Madras, Chennai, Tamil Nadu – 600 025, India *E-mail address: be20b029@smail.iitm.ac.in*

[7]Deptartment of ECE, College of Engineering, Guindy, Anna University, Chennai-600 025, India
E-mail address: meena68@annauniv.edu

Abstract

Multioperator multiservice support over mobile front haul networks would be an important requirement in the evolving 5G Wireless Communication architectures. This in turn dictates the need for high capacity and high connectivity front-haul options. Optical Code Division Multiplexing over Wavelength Division Multiple Access could be one of the most promising system architectures to support the last/first-mile bottleneck of the Mobile Networks. This paper reports a comparison impact of the energy efficiency and electromagnetic radiation effects for a multioperator multiservice OCDM-based Spectrally Amplitude Encoded Analog Radio over Fiber front-haul for a small cell configuration. The WDM multiplexed mm-wave signals at 60GHz and 28GHz and Prime code-based spectral amplitude patterns assigned for conventional services are analyzed and compared with the Wavelength Division Multiple Access system of the same kind. The comparison results confirm that the proposed architecture will be a suitable candidate to meet the 5G challenges of Mobile fronthaul Networks.

Keywords: *Green communication; Energy efficiency; Electromagnetic pollution; Fronthaul; Multi-operator multi-service, Radio over fiber*

1. Introduction

The evolving trend in the next generation of wireless communication suggests the increasing necessity for integrating different communication architectures, transport options, and switching technologies, to support the growing demand in the number of Internet users, bandwidth-intense applications, and the Internet of Things (IoT). Radio architecture is now evolving to provide operators with enhanced flexibility, capacity, coverage, and scalability (Lucent, 2012) &(NSN, 2013). Commercial mobile broadband networks are undergoing a dramatic transformation in their topology by implementing public access small cells which are the key for the future. Although

*Corresponding author

Received: 29th, June 2023, Revised: 04th September, 2023, Accepted: 18th September 2023 and available online 29th September 2023

This work is licensed under a Creative Commons Attribution 4.0 License(CC BY 4.0).
For more information, see https://creativecommons.org/licenses/by/4.0/

growth in demand is often cited as the key driver for small cells to provide increased capacity, technology is also approaching efficiency limits. To support the high-capacity users in the densely populated urban zone, many small cells (Naylon, 2013) need to be located to provide coverage.

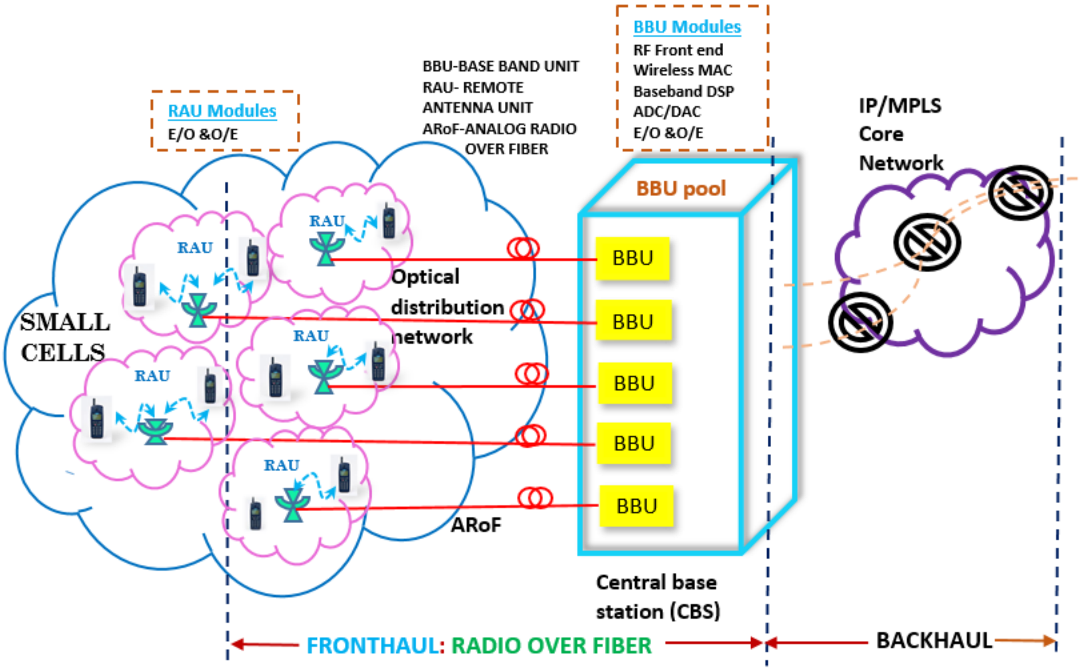

Figure 1. Architecture of small cell-based Cloud-RoF

The phenomenal growth of wireless connectivity is made possible today at the expense of considerable energy consumption, which in turn adds to carbon dioxide (CO_2) emissions and global warming problems (Amanna, 2011). With the advent of the data-intensive cellular standards, power consumption for each base station can increase up to 1,400 watts and energy costs per base station and can reach $3,200 per annum with a carbon footprint of 11 tons of CO_2 (Hasan et al., 2011). The rapidly growing demand for mobile communication technology has resulted in an exponential increase in the number of cellular BSs worldwide million a few hundred thousand to many millions within the last couple of years. Such a substantial jump in the number of BSs that power a cellular network account for the sudden increase in the Green House Gases (GHG) and pollution, in addition to higher energy costs to operate them (Correia et al., 2010). Recently, there has also been an ongoing debate about the associated health risks due to radiation from mobile equipment and BS towers (Kumar, 2010) Interphone study in 2010 mentions that excessive use of mobile phones has doubled to quadrupled brain tumor risk (Katiyar et al., 2012). Therefore, it is crucial to reduce the power consumed as well as the power radiated from the cellular networks (Nin, 2010).

The power amplifiers and the climate control units present in the base station (BS) of the cellular network consume more than 60% of the energy. A network architecture needs to be evolved in such a way as to avoid the usage of PAs. The small cell network (SCN) approach implemented with RoF-based fronthaul is expected to significantly reduce energy needs and the electromagnetic field exposure to the mobile user and his immediate neighbors as well as a larger pollution closer to the BS tower (Brindha and Meenakshi, 2015) & (Hoydis et al., 2011). The other factors driving operators to deploy small cells are their deployment styles and the type of back-haul and front-haul requirements. The exploration of higher RF bands, especially at the millimeter-wave (mm-Wave) band (30 GHz-300 GHz), has attracted huge attention from both industries and academia for their high bandwidth support. The combination of mm Wave radio and small-cell architecture (Naylon, 2013) provides a promising solution for next-generation very-high-speed wireless access networks. The main challenge is the RoF interface design to support mm Wave services as well as backward

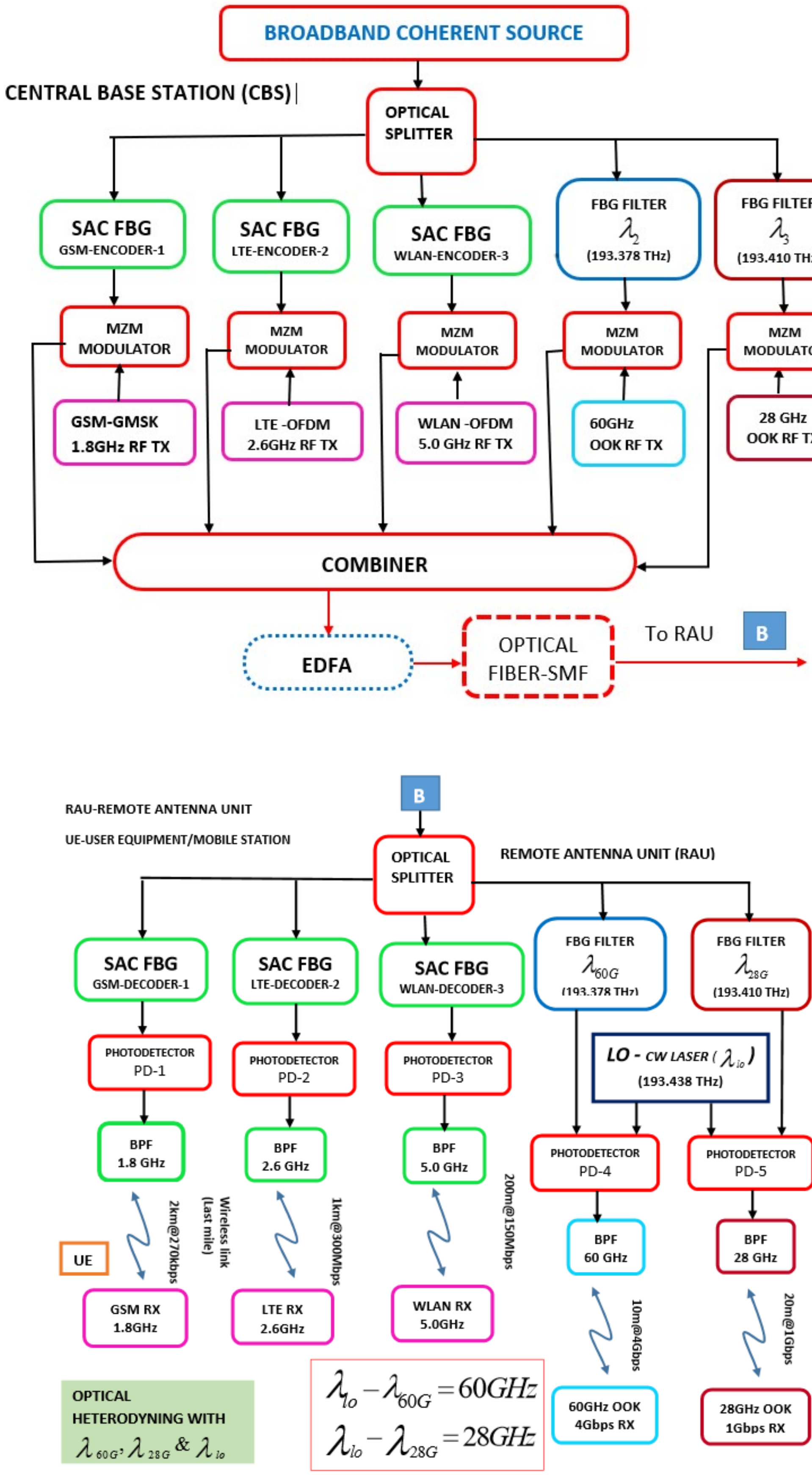

Figure 2. System block diagram of SAC-OCDM

compatibility with the legacy wireless services.

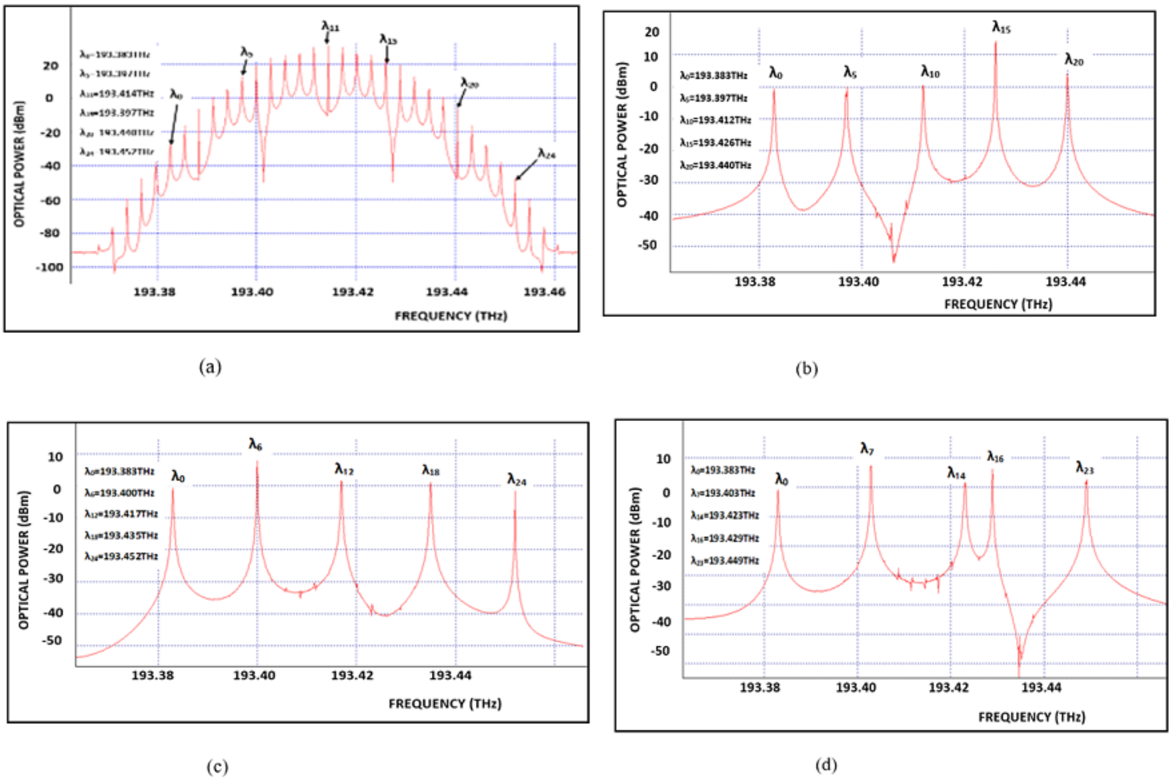

Figure 3. (a) Broadband coherent source emission spectrum (b) Spectral code pattern ($\lambda_0\lambda_5\lambda_{10}\lambda_{15}\lambda_{20}$) for GSM signal (c) Spectral code pattern ($\lambda_0\lambda_6\lambda_{12}\lambda_{18}\lambda_{24}$) for LTE signal (d) Spectral pattern ($\lambda_0\lambda_7\lambda_{14}\lambda_{16}\lambda_{23}$) for WLAN signal

Migrating to optical backhauling and fronthauling along with the adoption of small cell architecture is the way forward over the long-term solution to reduce GHG emissions because optical communications devices consume less energy than electronic ones. Network devices can also be designed with features that create an opportunity for energy-saving operation, such as turning off network interfaces and throttling of processors. The currently deployed fronthaul links are based on the Common Public Radio Interface (CPRI) protocol or the Open Base Station Architecture (OBSAI) Interfaces (Twe, 2013),(NI, 2017) & (Fou, 2014). The link supports digitized IQ samples of the radio signal, suitable preambles, and control information. The challenge in this approach is the scalability in link capacity to support multiplexed signals from the larger number of remote antenna systems. This constraint is even more stringent when multiple radio services or multiple operator's signals need to be simultaneously transmitted over the fiber fronthaul.

Analog radio-over-fiber (ARoF) method enables multi-service multi-operator coexistence in a shared infrastructure with simplified RAUs whereas the conventional digital-baseband-transmission approach typically supports only one service at a time. In addition, it is beneficial to integrate with optical wavelength division multiplexing (WDM) techniques to provide more versatility and flexibility to the fronthaul/backhaul networks. Such a system provides multiple operational advantages such as:

1. Multiple operators can co-exist in a shared small-cell infrastructure by using different WDM wavelengths.
2. Within each operator, different wireless services can co-propagate in the RoF fronthaul/backhaul in a simplified way.
3. For each wireless service, multiple MIMO data streams and multiple sub-bands can also coexist in the RoF link without incurring undesirable interference.

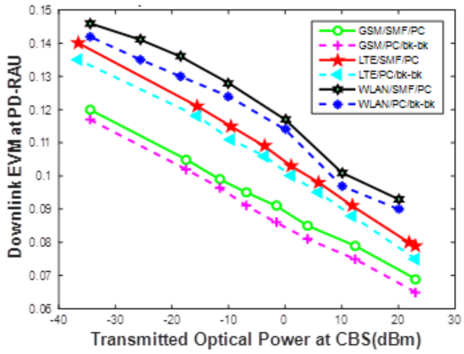

Figure 4. Comparison of the multiservice OCDM-PC of operator-1

4. Multiple operators, multiple services, and multiple wireless techniques can share the same small-cell infrastructure while maintaining independent reconfigurability through centralized management (Liu et al., 2013).

WDMA networks require stringent control over the optical wavelength spacing and filter bandwidth to accommodate individual operators/services on uniquely allocated optical channels. Moreover, the available wavelength resource in mainstream WDMA systems is also limited and there is a need to find alternate approaches for sharing the available spectrum without affecting the achievable bit rate. Hence, WDM cannot be brought down to the customer premises of small-to-medium sized businesses and residential users. Optical code division multiplexing (OCDM) layer over WDMA provides a possible solution. OCDM can provide access to connections on demand simultaneously, multiplexed at the same wavelength channel through unique signature codes (Cao and Qian, 1992) & (Prucnal, 2005). Such an OCDM option is explored in this paper to support multiple-operator multiservice provisioning using ARoF front haul.

(Zhang, 1999) proposed an Integrated Services Digital Broadcasting (ISDN) system employing a multirate optical code-division multiplexing technique in which unique one-dimensional optical orthogonal codes (OOCs) were used to represent the services. The authors using analytic and experimental results, concluded that the system can support Fast Ethernet up to 125 Mb/s, FDDI up to 125 Mb/s, ATM up to 155 Mb/s, and ESCON up to 200Mb/s protocol data. Because OCDMA technology can implement multiple asynchronous access at random and flexible diversity of encoding, in addition to effectively supporting data network, many types of media such as voice, data, image, and video, can be sustained in the communication link by the flexible network design and variety of choices of OCDMA systems.

(Kwong and Yang, 2002) proposed a kind of OCDMA network that provides appropriate quality of services (QoS) for different subscribers. For example, different service demands from different subscribers can be satisfied by encoding high-rate services with short codes and low-rate services with long codes, services with high QoS by codes with high performance, and low QoS by codes with low-performance codes. ARoF system based on the OCDMA multiplexing method was proposed in (Tsukamoto et al., 2003) in which the theoretical analysis and experimental demonstration were conducted. The unipolar prime code was employed in this system and the results reveal that the proposed scheme is effective. In addition, it was shown in theory that the number of maximum connected RBSs could be further improved by employing bipolar pseudo noise (PN) codes.

The main difference between the proposed paper and the previously published paper which we have cited in the reference section (Saminathan et al., 2017) is as follows:

1. Optical Code Division Multiplexing (OCDM) over Wavelength Division Multiple Access (WDMA) could be one of the most promising system architectures that can break through the last/first mile bottleneck of the Mobile Networks.

2. WDMA networks, which uniquely assign a wavelength to each user, can accommodate only a moderate number of users/operators/services.

3. Spectrally encoded OCDM can provide an additional degree of freedom by allowing multiple access connections simultaneously on a single WDMA channel. Multiple users of a single service/ multiple services of a single operator can be multiplexed on the same wavelengths through unique spectral signature patterns.

4. In the WDMA-based MOMS-AROF architecture (Saminathan et al., 2017) conventional services like GSM, LTE, and WLAN, are multiplexed and externally modulated at the same wavelength whereas in the proposed SAC-OCDM architecture exclusive patterns based on unique Prime codes are assigned for each service like GSM, LTE, and WLAN, encoded and multiplexed at the same wavelength.

5. The usage of unique prime codes (SAC-OCDM) reduces the system cost for multiple services of a single operator/handling of multiple users of a single service instead of allocating wavelengths (MOMS-AROF case).

The results of both system architectures suggest the possibility of eliminating the energy consuming power amplifiers (PA) in the transceivers to achieve reduced electromagnetic pollution in the environment, so MOMS-AROF can be replaced by SAC-OCDM to reduce the system cost.

The rest of the paper is organized as follows. In Section 2, SAC-OCDM architecture is discussed with 5 different services. In Section 3, Prime codes for SAC-OCDM are explored concerning multiservice. Section 4 presents in detail the link performance analysis and discussion. Section 5 contains the Link power budget, Energy considerations, and BER analysis for each service separately and then compared with the WDM backbone with appropriately assumed parameters. Finally, the conclusions are highlighted in Section 6.

2. SAC-OCDM Architecture

The small cells-based Cloud RoF architecture is depicted in Fig.1. The multioperator multiservice analog radio over fiber (SAC-OCDM) integrated architecture in a heterogeneous cellular configuration is shown in Fig.2. The conventional wireless services such as GSM, LTE, and WLAN utilizing SAC OCDM coexist with mm wave band signals at 28 GHz and 60 GHz. At the Central Base Station (CBS), the conventional RF carrier signals representing multiservice like 1.8 GHz GSM, 2.6 GHz LTE, and 5.0 GHz WLAN from core networks are processed and encoded using SAC OCDM techniques with unique spectral patterns (Shalaby, 1999) & (Wei et al., 2001) based on the prime codes (PC).

This integrated system incorporating SAC-OCDM along with WDMA for multiservice in the radio over fiber system affords flexible configuration for each service independently. The multiple spectral components needed for SAC OCDM are derived from a broadband coherent source is listed in Table 1.

The optical signal emitted from a coherent broadband light source is split into multiple copies for multiple services (Avrutsky et al., 1998). In this case, a super Gaussian laser source with a RIN value of -150 dB/Hz is considered to carry on the simulation work. The spectral components corresponding to the specific SAC pattern assigned for each service with code length $n = 25$ are chosen based on the prime codes (PC) and the encoding process is carried out by employing the FBGs (Huang et al., 2000) & (Yang and Kwong, 1995). In doing so, the spectral amplitude encoding based on the FBGs for each service is achieved (Meenakshi and Andonovic, 2005), (Meenakshi and Andonovic, 2006) & (Kitayama et al., 2006). With the assigned prime code pattern, a suitable number of FBGs are used to get the wavelength pattern for each of the proposed service with the FBG having notch filter super Gaussian order of '1' and two-sided bandwidth (-3 dB) of 0.1 GHz (0.008 nm) specifications. Three properties that need to be controlled in an FBG are the reflectivity, the bandwidth, and the side-lobe strength. The side-lobe strength can be varied to help with side-lobe suppression called apodization of the refractive index change. Apodised gratings offer a significant improvement in side-lobe suppression while maintaining reflectivity and

Table 1. Spectral Components for $N = 25$

S.No.	**Multi wavelength source** $n = 25$
1	λ_0=193.383 THz
2	λ_1=193.386 THz
3	λ_1=193.389 THz
4	λ_1=193.391 THz
5	λ_1=193.394 THz
6	λ_1=193.397 THz
7	λ_1=193.400 THz
8	λ_1=193.403 THz
9	λ_1=193.406 THz
10	λ_1=193.409 THz
11	λ_1=193.412 THz
12	λ_1=193.414 THz
13	λ_1=193.417 THz
14	λ_1=193.420 THz
15	λ_1=193.423 THz
16	λ_1=193.426 THz
17	λ_1=193.429 THz
18	λ_1=193.432 THz
19	λ_1=193.435 THz
20	λ_1=193.438 THz
21	λ_1=193.440 THz
22	λ_1=193.443 THz
23	λ_1=193.446 THz
24	λ_1=193.449 THz
25	λ_1=193.452 THz

narrow bandwidth. The two functions typically used to apodise an FBG are Gaussian and raised-cosine. The numerical parameters used in the link simulation study are listed in Table 2. External modulation in the optical domain is usually achieved with the help of an MZM device wherein one of the inputs is the user information (GSM, LTE, WLAN, or mm wave signals) and the second input is the laser signal from broad coherent laser source with a specific spectral pattern generated using FBG. The MZM having extinction ratio of -20.0 dB, Vpi value of 5.0 V, (-3 dB) bandwidth of 10.0 GHz and average power reduction due to power modulation is around 3 dB is proposed for simulation in this case.

The GSM signal is generated with a suitable RF source of 1.8 GHz carrier signal which is suitably Gaussian shift keying (GMSK) modulated and then intensity modulated with MZM in which the second input is the spectral pattern generated with the help of FBG for the GSM signal. Then, the externally modulated signal is routed to the WDM multiplexer for further transmission. The LTE and WLAN signals are OFDM modulated with suitable RF sources of 2.6 GHz carrier signal & and 5.0 GHz carrier signal respectively and then intensity modulated with MZM in which the second input is spectral pattern generated using prime code with the help of FBG for the LTE signal& WLAN signal.

The GSM signal is externally MZM modulated with a ($\lambda_0 0000$ $\lambda_5 0000$ $\lambda_{10} 0000$ $\lambda_{15} 0000$ $\lambda_{15} 0000 = (\lambda_0 \lambda_5 \lambda_{10} \lambda_{15} \lambda_{20})$ specific spectral pattern with indexed wavelengths as specified in Table 1. The procedure is repeated for LTE and WLAN with ($\lambda_0 0000$ $0\lambda_6 000$ $00\lambda_{12} 00$ $000\lambda_{18} 0$ $0000\lambda_{24} = (\lambda_0 \lambda_6 \lambda_{12} \lambda_{18} \lambda_{24})$ & $\lambda_0 0000$ $00\lambda_7 00$ $0000\lambda_{14}$ $0\lambda_{16} 000$ $000\lambda_{23} 0 = \lambda_0 \lambda_7 \lambda_{14} \lambda_{16} \lambda_{23}$), respectively. In doing so, the spectral amplitude encoding based on the FBGs for each service is achieved (Meenakshi and Andonovic, 2005), (Meenakshi and Andonovic, 2006) & (Kitayama et al., 2006).

The 60 GHz and 28 GHz data services offered by operator-2 and operator-3 use baseband on-off Keying (OOK) modulation and intensity modulate the wavelengths λ_{60G} (193.378 THz) and λ_{28G} (193.410 THz) respectively. A typical digital fiber transmission system makes use of the simplest method called Amplitude Shift Keying (ASK) or On–Off Keying technique wherein the voltage level is switched between two values that is ON and OFF to send digital message pulses i.e., the optical signal emerging from the transmitter binary 1 represented by the presence of light pulse and binary 0 by the absence of light pulse. This kind of simple modulation technique is implemented for mm wave signals like 60 GHz and 28 GHz to keep the system cost effective. The WDM multiplexed mm wave signals and the three spectrally encoded conventional signals are combined in an optical star coupler and transmitted through 25 km standard single mode fiber (SMF) connected between CBS and the RAUs. To keep the system simple and cost effective, the compensation of any optical domain impairment has to be done in the electronic domain with suitable signal processing adaptively depending on the necessity. At the remote antenna Unit (RAU) the signals would be wavelength de-multiplexed. The conventional wireless service signals are properly decoded using the assigned spectral pattern in their respective decoding units and then detected by a PIN photodetector (PD) receiver with a sensitivity of -36 dBm (Agrawal, 2010) for an allowed error probability of 10^{-9}. By proper selection of wavelengths, the crosstalk term will fall beyond the electrical bandwidth of receiver PD.

High-performance photodetectors are used in the proposed system which are capable of handling more than two signals at a time for the detection process. The allowed value lies between 0 and 1 and the default value is 0.75. The responsivity is related to quantum efficiency. Hence, the present approach for sharing channel resources enables infrastructure sharing among multiple operators without interference. A single PD has the power constraint of detecting signals on multiple wavelengths and hence the number of operators to share a single PD is limited (Liu et al., 2013). After photodetection, the multiple RF signals on different carrier frequencies like 1.8, 2.6, and 5.0GHz are filtered out using suitable bandpass filters (BPF) and transmitted wirelessly to mobile users (MU). The signals on wavelengths would coherently beat with a local optical source at wavelength λ_{lo} in their respective PDs, to generate the OOK modulated mm wave signals at 60 GHz and 28 GHz, respectively. The feasibility of such an approach has been reported in (Agrawal, 2010).

The last mile connectivity between RAU and UE varies for different services based on the data rate supported by that specific service. In the present work, GSM service with the minimum last mile wireless connectivity of 2 km with the data rate of 270 kbps (a single user), LTE user with the last mile connectivity of 1 km with the data rate of 300 Mbps, WLAN user with the last mile connectivity of 200m with the data rate of 150 Mbps, LMDS user with the last mile connectivity of 20m with the data rate of 1.0 Gbps and Wi-Gig user with the last mile connectivity of 10m with the data rate of 4 Gbps, is considered for the simulation study of multiservice operation and then justified with suitable wireless power budget analysis discussed in Section 5. At UE, the received analog signal is then detected with the respective demodulator circuits and the BER is estimated. A good quality of service is achieved with the specifications considered for all five services and different operators. A detailed power budget analysis is also done for all the services to determine the energy efficiency and a quantitative estimate for the possible electromagnetic pollution and discussed in Section 5.

3. Prime Codes for SAC-OCDM

The construction of a prime code (PC) is carried out as in (Kwong and Yang, 2002). Firstly, choose d as a prime number and based on the Galois field $GF(d)$, construct a prime sequence

$$PC_i = p_{i,0}, p_{i,1}, p_{i,2}, ...p_{i,j}, ...p_{i,(d-1)} \tag{1}$$

Where $i = 0, 1, 2, ...d - 1$

Where the element in this prime sequence is

$$p_{i,j} = \{i.j\}(mod\, d) \tag{2}$$

Table 2. Parameters Specifications

Parameters	**Value**
Broadband source emission wavelength range	1549.47927 nm-1550.52 nm
Broadband source emission frequency range	193.34949 THz-193.47949 THz
Operator-1-Service 1-GSM signal (at CBS)-Prime code spectral pattern (from Broadband source)	PC_0 =(00000) $=\lambda_0\lambda_5\ \lambda_{10}\lambda_{15}\lambda_{20}$ $=\lambda_0 0000\lambda_5 0000\ \lambda_{10}0000\lambda_{15}0000\lambda_{20}0000$
Operator-1-Service 2-LTE signal (at CBS)-Prime code spectral pattern (from Broadband source)	PC_1 =(01234) $=\lambda_0\lambda_5\ \lambda_{12}\lambda_{18}\lambda_{24}$ $=\lambda_0 0000\ 0\lambda_6 000\ 00\lambda_{12}00\ 000\lambda_{18}0\ 0000\lambda_{24}$
Operator-1-Service 3-WLAN signal (at CBS)-Prime code spectral pattern (from Broadband source)	PC_1 =(02413) $=\lambda_0\lambda_7\ \lambda_{14}\lambda_{16}\lambda_{23}$ $=\lambda_0 0000\ 00\lambda_7 00\ 0000\lambda_{14}\ 0\lambda_{16}000\ 000\lambda_{23}$
Operator-2-λ_{60G}(at CBS)	1550.29247 nm (193.378 THz)
Operator-3-λ_{28G}(at CBS)	1550.03598 nm (193.410 THz)
Local Oscillator-λ_{lo}(at RAU)	1549.81161 nm (193.438 THz)
$\lambda_{lo} - \lambda_{60G}$(Heterodyne at PD)	60 GHz)
$\lambda_{lo} - \lambda_{28G}$(Heterodyne at PD)	28 GHz)
Service 1-GSM signal	1.8 GHz-270Kbps-GMSK
Service 2-LTE signal	2.6 GHz-300Mbps-4-QAM-OFDM
Service 3-WLAN signal	5.0 GHz-150Mbps-4-QAM-OFDM
Service 4-Small cell-Wi-Gig	60.0 GHz-4.0Gbps-OOK-mm wave
Service 5-Small cell-LMDS	28.0 GHz-1.0Gbps-OOK-mm wave
Fiber length between CBS & RAU (SMF)	$\sim$ 28km
Distance between RAU & UE	$\sim$ 10m-20m-Small cell $\sim$ 200m-WLAN Up to 1km-LTE Up to 2km-GSM
Fiber dispersion (D)	16ps/nm/km
Fiber loss	0.2 dB/km
Receiver sensitivity	−36.0 dBm
Receiver Responsivity	0.8 A/W
channel type	AWGN (Rayleigh fading)

Table 3. The Prime code sequence

Elements of GF(5)	0 1 2 3 4
PC_0	0 0 0 0 0
PC_1	0 1 2 3 4
PC_2	0 2 4 1 3
PC_3	0 3 1 4 2
PC_4	0 4 3 2 1

$p_{i,j}.i\&j$ are the elements over the Galois field $GF(d) = (0, 1, 2....d-1)$. Then, with the prime sequence

$$C_{i,k} = \begin{cases} 1 & \text{if } k{=}p_{i,j} + j.w, \text{ for } j = (0, 1, 2....d-1) \\ 0 & \text{otherwise} \end{cases} \tag{3}$$

A binary prime code can be obtained as follows:

$$C_i = c_{i,0}, c_{i,1}, c_{i,2}, ...c_{i,k}, ...p_{i,(n-1)} \tag{4}$$

Where $i = 0, 1, 2, ...d-1,\ n = d^2$

The code length and code weight of the prime code are $n = d^2$ and $w = d$, respectively. The maximum autocorrelation side lobe and maximum cross-correlation value for this code are $\lambda_a = d-1$ and $\lambda_c = 2$, respectively (Yin and Richardson, 2009). The cardinality of PC is |C| =d. According to the definition of optical orthogonal code, PC is a quasi-OOC with the parameters $(n, d, \lambda_a, \lambda_c){=}(d^2, d, d{-}1, 2)$. The prime sequence PC_i and the prime code C_i constructed assuming $d = 5$ are shown in Tables 3 and 4. From Tables 3 and 4, it can be seen that each code word in a prime code can be divided into d subsets with the length d for each subset. There is exactly one "1" in each subset and the position of this "1" is determined by the element in the corresponding prime sequence. The advantage of the prime code is that its generation algorithm is very simple and the shortcomings are that it has larger autocorrelation side lobes equal to $d-1$, its cross-correlation is not always equal to 1 and the cardinality of the prime code is only equal to its weight. In this work, the perfect code synchronization is assumed so that the correlation issues are reduced and the cardinality is not a major issue because of considering only a lesser number of services.

Table 4. Spectral pattern for prime codes C_i constructed for $n = d^2$

Prime Sequence PC_i	**Prime Code** C_i
$PC_0 = (00000) = \lambda_0\lambda_5\ \lambda_{10}\lambda_{15}\lambda_{20}$	10000 10000 10000 10000 10000 $\lambda_0$0000 $\lambda_5$0000 λ_{10}0000 λ_{15}0000 λ_{20}0000
$PC_1 = (01234) = \lambda_0\lambda_6\ \lambda_{12}\lambda_{18}\lambda_{24}$	10000 01000 00100 00010 00001 $\lambda_0$0000 0$\lambda_6$000 00λ_{12}00 000λ_{18}0 0000λ_{24}0000
$PC_2 = (02413) = \lambda_0\lambda_7\ \lambda_{14}\lambda_{16}\lambda_{23}$	10000 00100 00001 01000 00010 $\lambda_0$0000 00$\lambda_7$00 0000λ_{14} 0λ_{16}000 000λ_{23}0
$PC_3 = (03142) = \lambda_0\lambda_8\ \lambda_{11}\lambda_{19}\lambda_{22}$	10000 00010 01000 00001 00100 $\lambda_0$0000 000$\lambda_8$0 0λ_{11}000 0000λ_{19} 00λ_{22}00
$PC_4 = (04321) = \lambda_0\lambda_9\ \lambda_{13}\lambda_{17}\lambda_{21}$	10000 00001 00010 00100 01000 $\lambda_0$0000 0000λ_9 000λ_{13}0 00λ_{17}00 0λ_{21}000

4. SAC-OCDM Link Performance Analysis and Validation

To validate and analyze the feasibility of the proposed architecture simulations are performed using RSoft-Optsim-V2015.06 (Thi, 2015) & (Hirata et al., 2008). With the help of quasi analytical method, the parameters bit error-rate (BER) and error vector magnitude (EVM) calculations are carried out. The minimum transmit power requirement to achieve a BER value of 10^{-9} to 10^{-12} at the RAU with a fiber length of 25 km for all proposed services along with the required receiver sensitivity are derived from the simulations carried out (Taniguchi et al., 2009), (theodore s. Rappaport, 2002) & (Tse and Pramod, 2005).

Table 5. The Prime code sequence

Component	Loss (dB)
FBG Filter (10×0.5)	5.0
Mux (5×1)	2.2
De-Mux (1×5)	2.2
SMF step index cable at 1550nm (25 km×0.2dB/km)	5.0
Splitter	1.5
External Modulator (MZM)	2.5
Coupler	1.5
System Margin	4.5
Fusion splicer (2×0.02)	0.04
Dispersion margin	1.0
SC Connector (2×0.5)	1.0
Total span loss	26.44

Table 6. Comparison of Observations

Scheme		**% of Useful power**	**Energy Spent/bit (Joules per bit)**	**% of Total area exposed to EMR**
Conventional Macrocell		3.5 %	1.44 $\times 10^{-3}$	0.12 %
Cloud RAN (CPRI Interface)		3.6 %	3.56 $\times 10^{-7}$	0.067 %
MOMS-ARoF	GSM	12.79 %	3.15 $\times 10^{-5}$	0.066 %
	LTE	12.79 %	8.3 $\times 10^{-9}$	0.068 %
	WLAN	12.79 %	7.7 $\times 10^{-10}$	2.39 %
	LMDS	12.87 %	3.3 $\times 10^{-11}$	0.068 %
	Wi-Gig	12.86 %	2.05 $\times 10^{-12}$	2.25 %
SAC-OCDM	GSM	12.87 %	7.93 $\times 10^{-6}$	0.016 %
	LTE	12.85 %	2.1 $\times 10^{-9}$	0.017 %
	WLAN	12.89 %	6.1 $\times 10^{-10}$	0.064 %
	LMDS	12.89 %	5.5 $\times 10^{-11}$	3.74 %
	Wi-Gig	12.86 %	2.6 $\times 10^{-12}$	2.8 %

The overall emission spectrum of the broadband coherent source is depicted in Fig.3(a), where only 25 wavelengths ($\lambda_0....\lambda_{24}$) from 193.383 THz to 193.452 THz are considered to represent the prime code for different services. The range of spectral code patterns representing unique prime code for the GSM signal of operator-1 derived from a broadband coherent source at CBS is depicted in Fig.3(b). similarly for LTE signal of operator-1 spectral code pattern ($\lambda_0\lambda_6\lambda_{12}\lambda_{18}\lambda_{24}$) and WLAN signal of operator-1 spectral code pattern ($\lambda_0\lambda_7\lambda_{14}\lambda_{16}\lambda_{23}$) are depicted in Fig.3(c) & (d), respectively. Each of the conventional services of operator-1 is analyzed and compared using the SAC-OCDM technique based on the prime codes. The downstream data rates range from 270 Kbps to 300 Mbps for the 3 services considered. The transmitting power at a central base station (CBS) varies from -30 dBm to about 40 dBm for the 3 services by all three operators. The downstream traffic signal-to-noise ratio (SNR) for each service at PD output at RAU is evaluated and the corresponding EVM values are estimated using the SNR for both, the back-to-back link and the 25 km SMF link. The transmitted optical power is varied and performance is analyzed for each conventional services of operator -1 and plotted in Fig.4(a). In each service, 1.5dB to 3 dB improvement is observed for SAC-OCDM-based implementation. The BER estimated for the back-to-back case without a fiber link is also shown for comparison. The bk-bk (back-to-back) response is determined by directly connecting the outputs of the WDM MUX unit which is available at

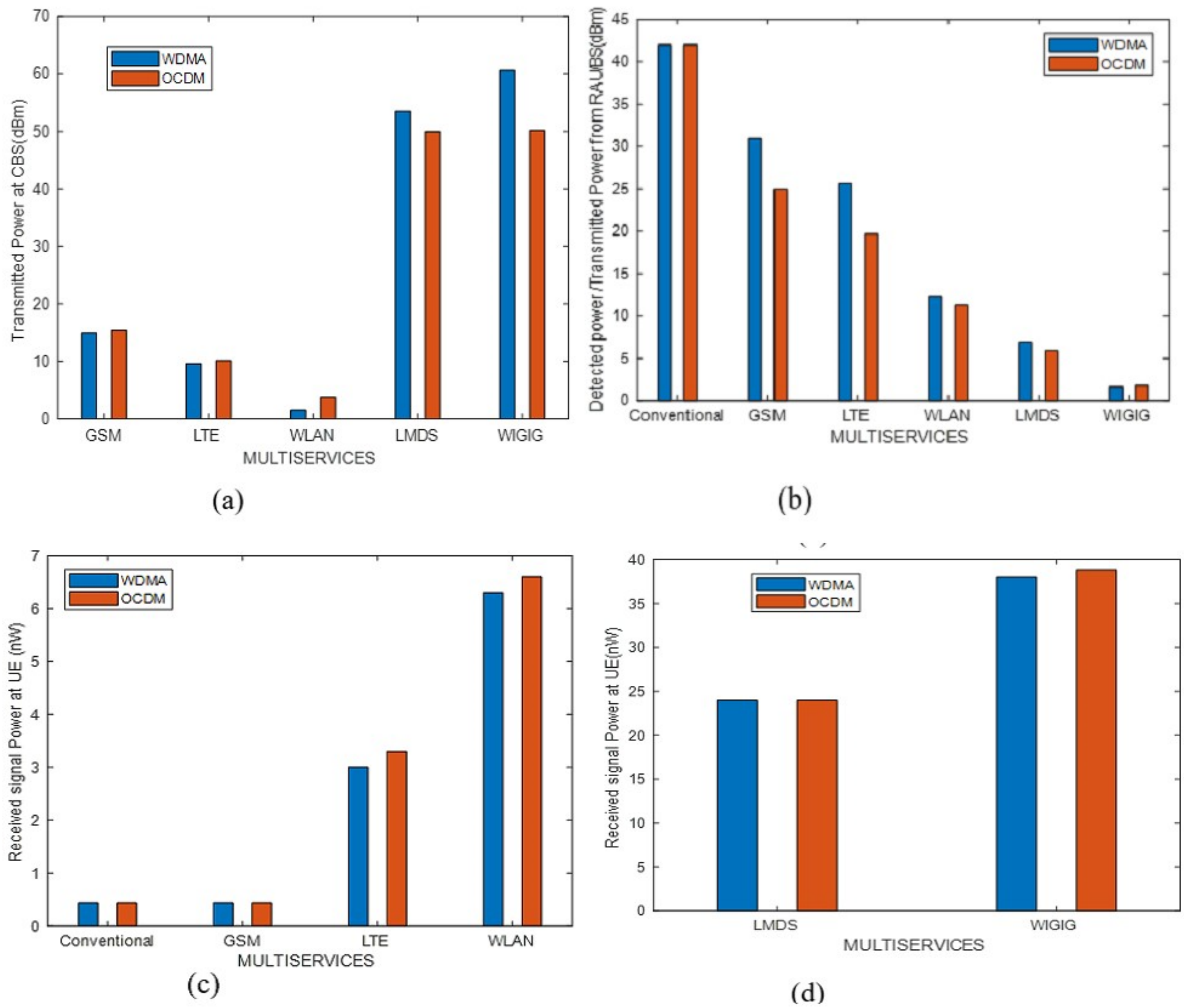

Figure 5. (a) Comparison of all 5 services at CBS for TX. Power (b) Comparison of all 5 services at RAU for Detected Power (c) Comparison of the services at UE for received signal power (d) Comparison of the mm wave services at UE for received signal power

the CBS (Central Base Station) to the WDM DEMUX unit of the RAU The bk-bk connectivity eliminates the data transmission through fiber or else the analysis is carried out between CBS and RAU without fiber connectivity in the proposed downstream scenario of the system.

5. Comparison of Link Power Budget, Energy Efficiency, and Electromagnetic Pollution Effect Analysis

The link power budget analysis for the entire RoF link is carried out based on the method discussed in (Saminathan et al., 2017), (Chen et al., 2018) & (Imtiaz et al., 2017) and compared for performance analysis with the WDMA system. The factors that constitute a span loss of 26.44 dB (Agrawal, 2010) for the SAC-OCDM system include all the parameters listed in Table 5.

From the power budget calculations (Saminathan et al., 2017) for SAC-OCDM-based services, it is observed that the minimum optical power required for GSM service over fiber is nearly 15.41 dBm at the CBS to achieve a BER of 10^{-4} in the user equipment (UE) with a fiber link distance of 25km and a wireless link distance of 1km. Similarly, for other services namely, LTE, WLAN, Wi-Gig, and LMDS, the minimum required optical power at CBS is found and the power budgets for all services are estimated and compared with the WDMA system as depicted in Fig.5(a). The detected power at RAU-PD for each service as well as the received power at each UE is measured and compared with the WDMA system as shown in Fig.5(b),(c) & (d). The percentage of total power consumed

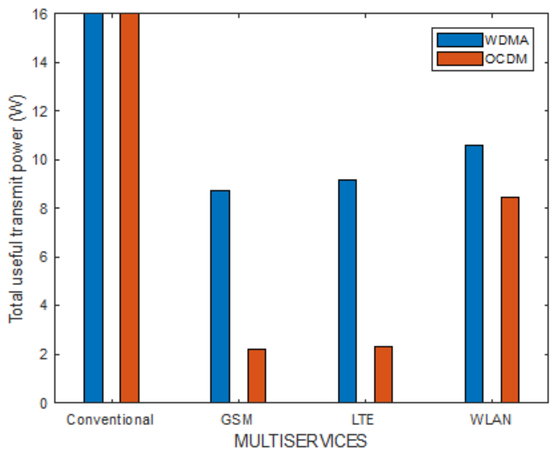

(a)

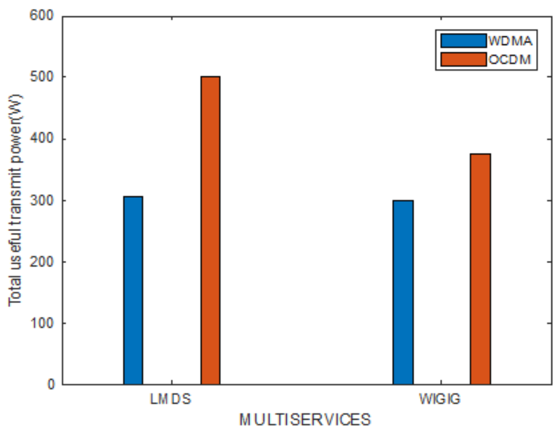

(b)

Figure 6. a) & (b) Comparison of the services for total useful Power

that is sent over the air as useful power, the energy spent per bit in units of Joules/bit (J/b), and possible electromagnetic pollution impact distance are estimated and analyzed. The minimum power that needs to be transmitted by the Remote Antenna Unit (RAU) for the RoF link so that the UE can detect the signal at the required BER level is calculated for all the services based on the methodology implemented in (Saminathan et al., 2017). The individual comparison of each service based on the prime codes-based on the SAC-OCDM and WDMA are analyzed and compared in the following sections. In the case of the conventional wireless link, a transmit power of 16 W is

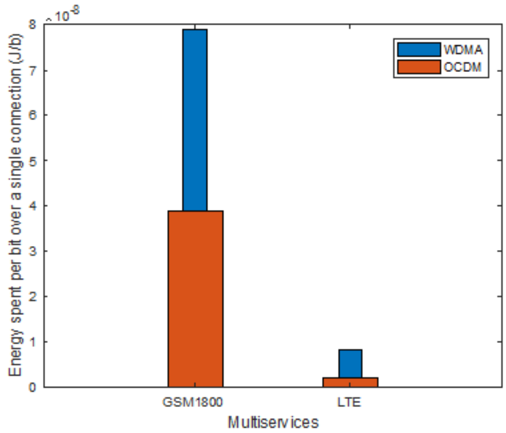

(a)

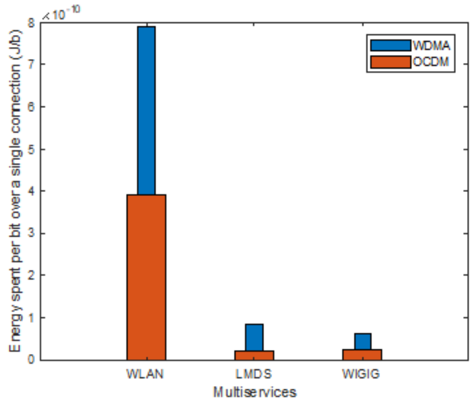

(b)

Figure 7. (a) & (b) Comparison of the services for energy spent per bit over a single connection

considered for a single data connection at 270 kbps over a 200 kHz channel bandwidth (Keiser, 2013) & (Thi). All the above losses are considered and the total power consumption is arrived at 447 W. The percentage of useful power works out to 3.5%. When the LTE service is operated over an SAC OCDM combine, the transmit power requirement at a single RAU is only 0.63W and the total requirement to cover the region with 25 RAUs is 2.3W. The total power consumption at the RAUs is 17.9 W. The percentage of useful power in this case works out to 12.87% which is significantly higher as compared to the conventional single BS wireless scenario. The calculations carried out for the other services also show similar improvement as depicted in Fig. 6(a) & (b).

The energy spent per bit is calculated based on the grid power required at the BS/RAU for a single connection. Here again, it is noted that the energy spent per bit in the conventional scenario is 1.44 mJ/b, whereas for the AroF-based transmission of LTE, it is only 2.1 nJ/b. The corresponding values for the other services are also estimated and depicted in Fig.7(a) & (b). All the 5 services show a significant reduction in the energy spent per bit. Hence by using ARoF link with RAUs, the total power consumption can be significantly reduced despite provisioning high data rates. The possible electromagnetic pollution is compared by estimating the distance from BS/RAU up to which the power spectral density is above the threshold limit of 170 W/km^2 (Arnold et al., 2010). The comparison of the 5 services over ARoF is done with that of a conventional wireless service and the possible area of EMR exposure for each service is identified and depicted in Fig. 8(a). The percentage of the total area that has exposure beyond the threshold value is also compared for all the five ARoF services and the conventional scenario as depicted in Fig. 8(b), (c) & (d). It is observed that the AroF-based wireless services like GSM, LTE and WLAN expose less than 0.1 % percentage of the total area to EMR as compared to the conventional case where there is exposure for less than 1% of the total area. However, the millimeter wave services are observed to expose more than 2.5% of the total area to EMR. This is under the assumption that all the RAUs are actively transmitting (Venkatapathy et al., 2012). This means that the data rates supported in the region by these services is enormous and could be traded off for reduced EMR exposure. Table

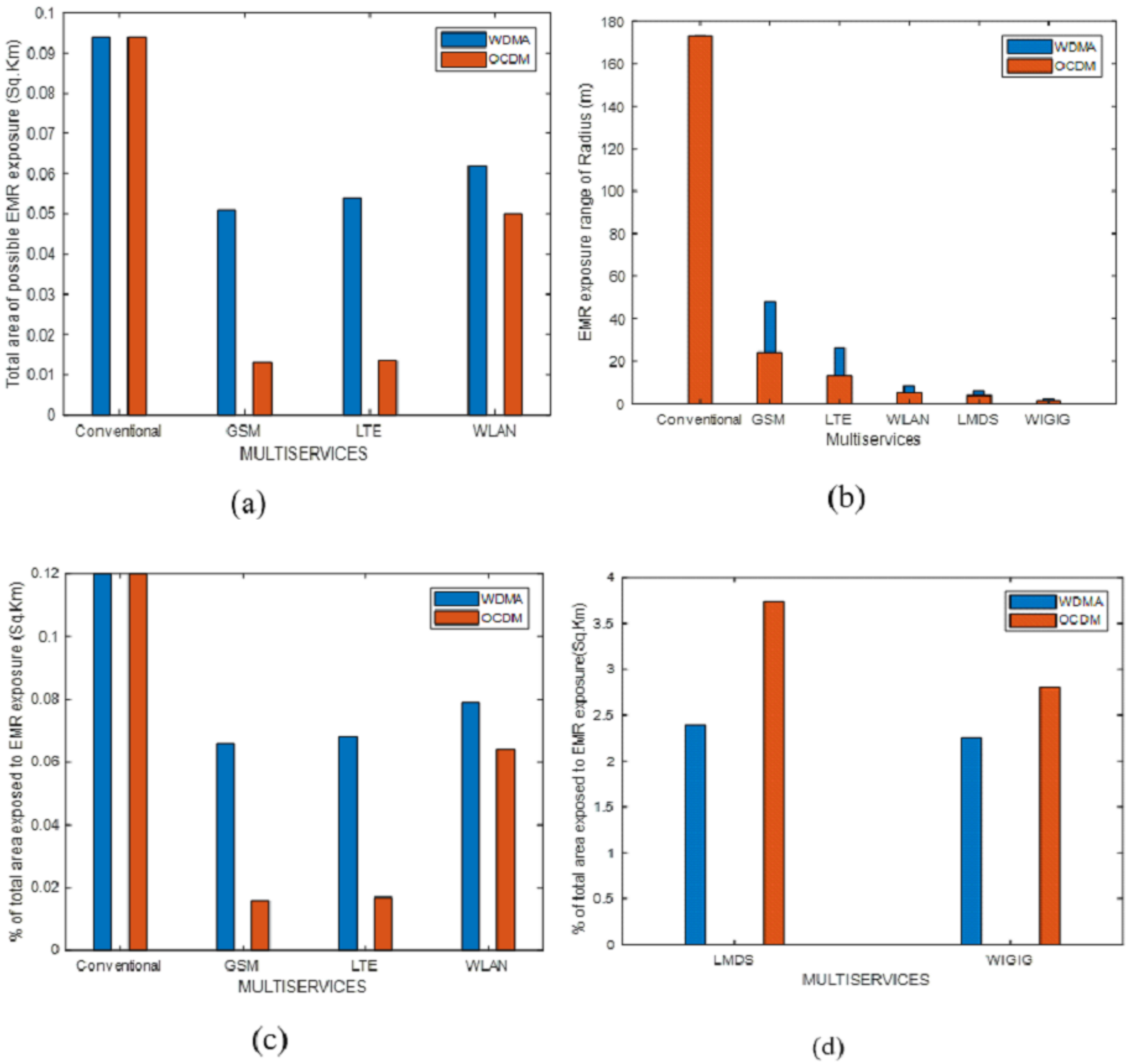

Figure 8. (a) Comparison of the services for total area exposed to possible EMR exposure, (b) Comparison of the services at UE for EMR exposure range of radius, (c) and (d) Comparison of the services for % of total area exposed to EMR exposure

6 presents the contributions of the proposed analog RoF and small cell network-based different architectural approaches that address energy efficiency, network capacity and the electromagnetic pollution aspects. The discussed energy and EMR considerations consolidated in Table 6 are a significant motivation to adopt SAC OCDM-based wireless access, although the deployment cost

may show some increase. However, the increased cost is offset by the sharing of resources as well as by making the entire system flexible and future proof. It is observed that AroF-based wireless services such as GSM, LTE and WLAN expose less than 0.1 % percentage of the total area to EMR.

6. Conclusion

Multioperator multiservice OCDM-based spectrally amplitude encoded analog radio over fiber (SAC-OCDM) fronthaul for a small cell configuration is suggested as a solution to reduce the system cost by employing suitable codes for multiple services instead of allocating wavelengths. Because OCDM can provide connections on demand to simultaneously employ the same lambda channels in appropriately coded forms, different services can be multiplexed at the same wavelengths through unique spectral signature patterns. Exclusive patterns based on the unique prime codes are assigned for each service like GSM, LTE, and WLAN, encoded and multiplexed at the same wavelengths. The comparison results of energy efficiency and electromagnetic pollution impact for the services confirm that the proposed architecture can meet the 5G fronthaul challenges.

7. Future Scope

Given the current trend and the rapid evolution of communication technologies, the future scope of this proposed work can be envisioned in the following areas such as Integration with 6G and Beyond, As the world moves towards 6G and beyond, the demand for efficient and cost-effective fronthaul solutions will only increase. The proposed SAC-OCDM architecture can be further refined and adapted to meet the requirements of future generations of wireless communication. Also, with the proliferation of IoT (Internet of Things) devices, there will be a need for efficient multiplexing solutions that can handle the massive data generated by these devices. The SAC-OCDM architecture can be optimized for IoT traffic. As multiple services are multiplexed at the same wavelengths, there might be concerns about crosstalk and potential eavesdropping. Future work can focus on enhancing the security aspects of the SAC-OCDM system. Given the emphasis on energy efficiency and reduced electromagnetic pollution, future research can delve deeper into making the SAC-OCDM system even more energy-efficient; thereby, contributing to sustainable and green communication solutions. As the number of services and the volume of data increase, the SAC-OCDM system should be scalable to handle this growth. Future work can focus on the scalability aspects, ensuring that the system can efficiently handle increased loads without compromising the performance.

References

Fiber optic testing. URL www.thefoa.org/tech/ref/basic/test.html.

Vodafone group plc, sustainability report, 2010. URL https://www.vodafone.com/content/dam/vodcom/sustainability/pdfs/2010-11_vodafone_sustainability_report.pdf.

Obsai specification, 2013. URL https://www.obsai.com.

Cpri interface specification, 2014. URL http://www.cpri.info/downloads/CPRI_v_6_1_2014-07-01.pdf.

Rsoft optsim v2015.06 user manual, 2015. URL http://optics.synopsys.com.

Agrawal, G. P. *FIBER-OPTIC COMMUNICATION SYSTEMS, Third Edition*. 2010. ISBN 978-81-265-1386-4.

Amanna, A. Green communications - annotated literature review and research vision. *White paper*, 2011.

Arnold, O; Richter, F; Fettweis, G, and Blume, O. Power consumption modeling of different base station types in heterogeneous cellular networks. 2010.

Avrutsky, I. A; Fay, M, and Xu, J. M. Multiwavelength diffraction and apodization using binary superimposed gratings. *IEEE Photonics Technology Letters*, 10, 1998. ISSN 10411135. doi: 10.1109/68.681503.

Brindha, S and Meenakshi, M. Radio over fiber system architecture: A boon to meet future energy and pollution challenges. *Optoelectronics and Advanced Materials, Rapid Communications*, 9, 2015. ISSN 20653824.

Cao, Z and Qian, Y. *The principle of modern telecommunication*. Tsinghua University Press, 1992.

Chen, K. S; Chen, Y. C, and Liao, L. G. Advancing high-speed transmissions over ocdma networks by employing an intelligently structured receiver for noise mitigation. *Applied Sciences (Switzerland)*, 8, 2018. ISSN 20763417. doi: 10.3390/app8122408.

Correia, L. M; Zeller, D; Blume, O; Ferling, D; Jading, Y; Gódor, I; Auer, G, and Perre, L. V. D. Challenges and enabling technologies for energy aware mobile radio networks. *IEEE Communications Magazine*, 48, 2010. ISSN 01636804. doi: 10.1109/MCOM.2010.5621969.

Hasan, Z; Boostanimehr, H, and Bhargava, V. K. Green cellular networks: A survey, some research issues and challenges, 2011. ISSN 1553877X.

Hirata, A; Takahashi, H; Yamaguchi, R; Kosugi, T; Murata, K; Nagatsuma, T; Kukutsu, N, and Kado, Y. Transmission characteristics of 120-ghz-band wireless link using radio-on-fiber technologies. *Journal of Lightwave Technology*, 26, 2008. ISSN 07338724. doi: 10.1109/JLT.2008.925641.

Hoydis, J; Kobayashi, M, and Debbah, M. Green small-cell networks. *IEEE Vehicular Technology Magazine*, 6, 2011. ISSN 15566072. doi: 10.1109/MVT.2010.939904.

Huang, W; Nizam, M. H; Andonovic, I, and Tur, M. Coherent optical cdma (ocdma) systems used for high-capacity optical fiber networks-system description, otdma comparison, and ocdma/wdma networking. *Journal of Lightwave Technology*, 18, 2000. ISSN 07338724. doi: 10.1109/50.848384.

Imtiaz, W. A; Qamar, A; Rehman, A. U; Ali, H; Chaudhry, A. R, and Iqbal, J. Design and analysis of self-healing tree-based hybrid spectral amplitude coding ocdma system. *Security and Communication Networks*, 2017, 2017. ISSN 19390122. doi: 10.1155/2017/2524513.

Katiyar, S; Jain, R. K, and Agrawal, N. K. R.F. Pollution Reduction in Cellular Communication. *arXiv e-prints*, art. arXiv:1204.1789, 2012. doi: 10.48550/arXiv.1204.1789. URL https://ui.adsabs.harvard.edu/abs/2012arXiv1204.1789K.

Keiser, G. *Optical fiber Communication*. Tata Mcgraw Hill, India, 2013. ISBN 978-1-25-900687-6.

Kitayama, K. I; Wang, X, and Wada, N. Ocdma over wdm pon - solution path to gigabit-symmetric ftth. *Journal of Lightwave Technology*, 24, 2006. ISSN 07338724. doi: 10.1109/JLT.2006.871030.

Kumar, G. Report on cell tower radiation, dot, delhi, 2010. URL https://www.ee.iitb.ac.in/~mwave/GK-cell-tower-rad-report-DOT-Dec2010.pdf.

Kwong, W. C and Yang, G. C. Design of multilength optical orthogonal codes for optical cdma multimedia networks. *IEEE Transactions on Communications*, 50, 2002. ISSN 00906778. doi: 10.1109/TCOMM.2002.801499.

Liu, C; Zhang, L; Zhu, M; Wang, J; Cheng, L, and Chang, G. K. A novel multi-service small-cell cloud radio access network for mobile backhaul and computing based on radio-over-fiber technologies. *Journal of Lightwave Technology*, 31, 2013. ISSN 07338724. doi: 10.1109/JLT.2013.2274193.

Lucent, A. lightradio network: A new wireless experience. *White paper*, 2012.

Meenakshi, M and Andonovic, I. Effect of physical layer impairments on sum and and detection strategies for 2-d optical cdma. *IEEE Photonics Technology Letters*, 17, 2005. ISSN 10411135. doi: 10.1109/LPT.2005.843935.

Meenakshi, M and Andonovic, I. Code-based all optical routing using two-level coding. *Journal of Lightwave Technology*, 24, 2006. ISSN 07338724. doi: 10.1109/JLT.2006.870962.

Naylon, J. Breaking barriers for small cell networks. *White paper*, 2013.

NI, . Efficient testing of wireless radio equipment including rf and cpri. *White paper*, 2017.

NSN, . Outdoor 3g/lte small cells deployment strategy: 'the race to the pole'. *White paper*, 2013.

Prucnal, P. *Optical code division multiple access: Fundamentals and applications*. 2005.

Saminathan, B; Tamilarasan, I, and Murugappan, M. Energy and electromagnetic pollution considerations in arof-based multi-operator multi-service systems. *Photonic Network Communications*, 34, 2017. ISSN 15728188. doi: 10.1007/s11107-017-0686-z.

Shalaby, H. M. Synchronous fiber-optic cdma systems with interference estimators. *Journal of Lightwave Technology*, 17, 1999. ISSN 07338724. doi: 10.1109/50.803019.

Taniguchi, T; Sakurai, N; Kimura, H, and Kumozaki, K. Technical trends in millimeter-wave band radio-on-fiber access system. volume 1, 2009. doi: 10.2529/piers080905073512.

theodore s. Rappaport, . *Wireless Communications Principles and Practice second edition*. 2002.

Tse, D and Pramod, V. *Fundamentals of wireless communication*, volume 9780521845274. 2005. doi: 10.1017/CBO9780511807213.

Tsukamoto, K; Higashino, T; Nakanishi, T, and Komaki, S. Direct optical switching code-division multiple-access system for fiber-optic radio highway networks. *Journal of Lightwave Technology*, 21, 2003. ISSN 07338724. doi: 10.1109/JLT.2003.819789.

Venkatapathy, P; Jena, J, and Jandhyala, A. Electromagnetic pollution index - a key attribute of green mobile communications. 2012. doi: 10.1109/GREEN.2012.6200932.

Wei, Z; Shalaby, H. M, and Ghafouri-Shiraz, H. Modified quadratic congruence codes for fiber bragg-grating-based spectral-amplitude-coding optical cdma systems. *Journal of Lightwave Technology*, 19, 2001. ISSN 07338724. doi: 10.1109/50.948274.

Yang, G. C and Kwong, W. C. Performance analysis of optical cdma with prime codes. *Electronics Letters*, 31, 1995. ISSN 00135194. doi: 10.1049/el:19950202.

Yin, H and Richardson, D. J. *Optical code division multiple access communication networks: Theory and applications*. 2009. doi: 10.1007/978-3-540-68468-8.

Zhang, J. G. Design of integrated services digital broadcasting systems using multirate optical fiber code-division multiplexing. *IEEE Transactions on Broadcasting*, 45, 1999. ISSN 00189316. doi: 10.1109/11.796270.